

COMPUTATION MODEL OF SHIELDING EFFECTIVENESS OF SYMMETRIC PARTIAL FOR ANTI-ELECTROMAGNETIC RADIATION GARMENT

Xiuchen Wang^{*}, Zhe Liu, and Mingli Jiao

Zhongyuan University of Technology, Zhengzhou, Henan 450007, P. R. China

Abstract—Current shielding effectiveness (SE) of electromagnetic shielding (EMS) fabric is tested in the plane state, the testing results are difficult to describe the shielding effect of a garment in a curve surface state after manufactured by the fabric. To solve this problem, this study proposes a new SE computation model of the EMS fabric based on a SE vector. The model can calculate a theoretical SE value of the EMS fabric in the curve surface state. A number of factors which determine the SE of the fabric with a curve surface are analyzed according to the principle of the reflection and transmission of the electromagnetic wave. This study also gives a new argument that the curve fabric can be divided into many micro-planes and the fabric SE is considered as a vector. And then a computation model of the SE of the curve fabric is constructed. The detail of computation is deduced, and an application example is given. Results of experiments and analyses show that the method is scientific and correct, and the error between the computation SE value and the testing SE value of the local garment is less than 3%. The model provides a new way to calculate the SE of the EMS fabric with symmetric curved surface.

1. INTRODUCTION

It is well known that the electromagnetic radiation pollutants have brought great harm to the human health. Therefore, the research on electromagnetic shielding (EMS) fabric and garment becomes a popular topic [1]. The main indicator for the shielding effect evaluation of the EMS fabric and garment is shielding effectiveness (SE). However, the value of the SE is all obtained by experiments such as far-field

Received 11 November 2012, Accepted 7 December 2012, Scheduled 10 December 2012

* Corresponding author: Xiuchen Wang (nbwangxiuchen@163.com).

testing, near-field testing and shielding enclosure [2]. These methods process two disadvantages. One is the testing fabric is in the plane state, so the fabric with curved surface state is not considered after the fabric is manufactured to garment. The other is the fabric is tested under a closed state condition, the fabric with a number of holes and interstices is not considered after fabric becomes garment. Therefore, it is difficult to describe the shielding effect of the curved surface fabric in actual wearing by the testing results of the plane fabric. It is a new problem to study the SE of the whole and local garment in wearing.

It is unrealistic that the SE evaluation of garment is obtained by the experiments because garment styles are changed. Moreover, there is not a mature testing equipment to test the garment. It will undoubtedly be a meaningful work that the SE of the garment local can be evaluated and calculated according to the SE of the fabric and the local shape of garment, and then the whole shielding effect of the garment is evaluated.

However, few of the studies focused on the SE of garment local. A number of scholars have explained the similar view. They all considered that the SE of fabric couldn't describe the SE of the clothing and the SE of clothing should be obtained according to the characteristic of each garment part [3, 4]. Kurokawa and Sato [5] and Yoshimura et al. [6] have studied the feature of the SE of the EMS clothing by the time domain measurements and the FDTD analysis. They constructed and derived the SE functions of the clothing on the point to the point along the curved surface of the body. We also have done a long-term research [7]. We have described the framework of the SE computation of the garment. In addition, a number of studies focus on the EMS fabric and textile products, such as model construction of blended EMS fabric [8, 9], performance analyses of blended EMS fabric [10, 11], computation of blended EMS fabric [12, 13], and influence factors analyses of blended EMS fabric [14, 15]. Sufficient information about the SE of products in other fields can be found in literature [16–19]. These studies provide reference for understanding, but do not apply to the EMS garment.

In general, the study on the SE of the garment local has not obtained some mature achievements at present. After long-term study, we consider that the SE of the garment is related with not only the fabric but also the local shape of the garment. The SE of the fabric should be combined with the garment local shape to construct a suitable computation model for the SE of the garment local. Therefore, we start from the simple symmetric local shape to discuss the SE computation of the garment local

To exactly evaluate the shielding effect of the symmetric local

of the garment, this paper proposes a new SE model of garment symmetric local based on the SE vector. The curved surface of the fabric is divided into a number of micro-plane regions with the SE vectors. The SE of a point is calculated by decomposing the SE vectors of the micro-plane and combining the curved surface shape. A SE computation model of the fabric with curved surface is built. Then the computation results are compared to the testing results. The comparison results show that this model can calculate the SE of the symmetric local of garment successfully.

2. MODEL DEVELOPMENT IDEAS

The SE is a shielding effect measure of the fabric on the electromagnetic wave. In the actual testing, the SE of the fabric is calculate as [15]

$$S = 20 \lg \frac{U_0}{U_S} \quad (1)$$

where, U_0 is the amplitude of one frequency point without shield and U_S the amplitude of one frequency point with shield

Let the electromagnetic wave be incident to a random plane fabric at a certain angle. The fabric is considered as an ideal shield. According to the distance between the emission source of the electromagnetic wave and the shield, the SE of fabric is discussed through two cases, including near field and far field. The theoretical model of the fabric SE in the far field is expressed as follows [20]:

$$SE_{far} = 168.16 - 10 \lg \frac{u_r f}{\sigma_r} + 1.31t \sqrt{f u_r \sigma_r} \text{ (dB)} \quad (2)$$

The theoretical model of the fabric SE in the near field is expressed as follows:

$$SE_{near} = 321.7 - 10 \lg \frac{u_r f^3 \gamma^2}{\sigma_r} + 1.31t \sqrt{f u_r \sigma_r} \text{ (dB)} \quad (3)$$

where t denotes the thickness of an idea shield (cm), μ_r the relative magnetic permeability, σ_r the relative conductivity, f the frequency (H_z), and γ the distance between the shield and the source of the magnetic field (cm).

As can be seen from Equations (2) and (3), the shielding effect of an ideal fabric shield is determined by the relative magnetic permeability, the relative conductivity and the thickness of the fabric as the frequency and the emission distance are unchanged. However, those three factors are determined by the content of metal fiber among yarns and the weave structure of the fabric. The fabric local shows

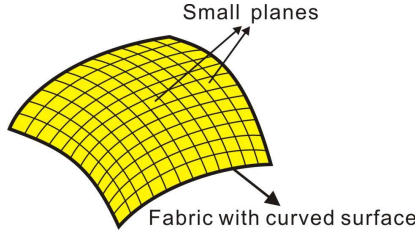


Figure 1. Micro plane of fabric with curved surface.

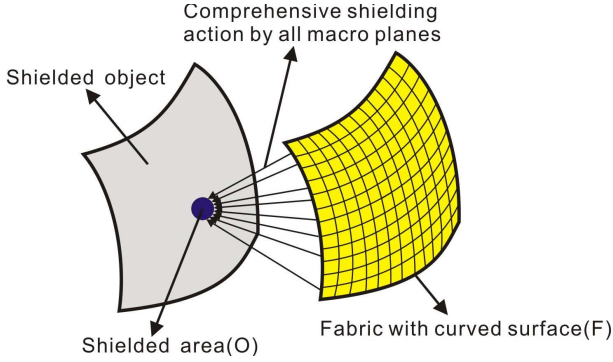


Figure 2. Comprehensive shielding action of the fabric with curved surface.

the curved surface state after it becomes the clothing, as shown in Figure 1. The fabric local can be considered as a constitution with many small planes. We call those small planes as macro planes. For a macro plane of the ideal fabric that is even and no extent, when the micro plane is small enough to become a point, and the emission distance and the frequency are stable, the point SE cannot be changed because the yarn and the fabric structure is not changed. Therefore, the SE of each point is same when the fabric is in a curved surface.

The local shielding effect of the clothing depends on a number of points on the curved surface of the fabric. As shown in Figure 2, F is the shielding fabric with curved surface; O refers to any point shielded by the EMS fabric F . Multiple micro planes undertake the shielding task when the electromagnetic wave is incident to the fabric F . The shielding effect of the point O is determined by the comprehensive shielding action of multiple micro planes. If the position between the point O and the fabric F is different, the shielding effect by the fabric F is different.

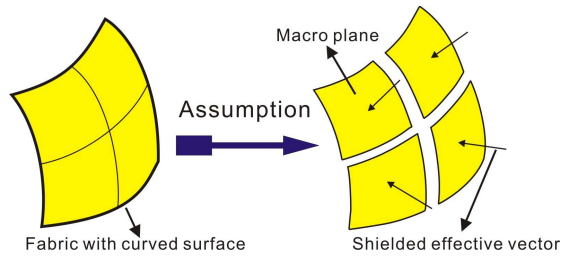


Figure 3. Comprehensive SE model of the fabric with curved surface.

Therefore, the following assumptions are given:

- 1) There is a vertical SE vector corresponding to each micro plane of the fabric with curved surface.
- 2) The comprehensive shielding effect of a point on a EMS object is determined by the SE vector of this point.
- 3) The SE vector of each micro plane in the fabric is same when the emission frequency and the emission distance are stable.

According to the three conditions mentioned above, we construct a comprehensive SE computation of the curved surface fabric based on the SE vector, and the model is verified by experiments. Figure 3 shows the diagram of the model. The curved surface consists of some small micro planes. Each micro plane is corresponding to a SE vector. The direction of the SE vector is vertical to the plane, and the value of the SE vector is the testing SE value of the fabric in a plane state.

3. COMMON COMPUTATION OF SYMMETRIC PARTIAL

According to model description mentioned above, we first discuss the SE computation of the curve surface fabric through some simple symmetric partials. The symmetric partial can describe a number of enclose areas with the symmetric partial characteristic on the human body such as chest, waist, and arm areas. As shown in Figure 4, let the curve surface of the EMS fabric be Π , the surface is uniform and smooth, and the parameter equation can be expressed as follows:

$$\begin{cases} x = \varphi(t) \\ y = \phi(t) \\ z = \omega(t) \end{cases} \quad (4)$$

The curve surface Π consists of many micro-plains. Let S_i be the i th plain. The SE vector corresponding to each micro-plain is SE_i ; its direction is vertical to the micro-plain; its value is the testing SE

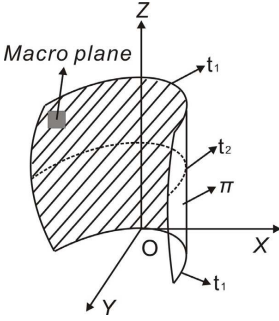


Figure 4. Ideal symmetric partial II.

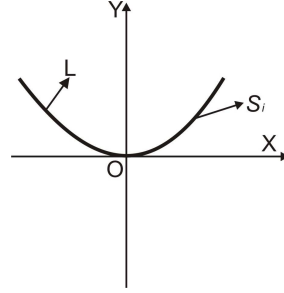


Figure 5. Projection curve L formed by the projection of the curve surface on the XOY coordinates.

of the fabric in a plain state. The curve surface II processes three sections: upper section, middle section, and lower section. The upper and lower sections are the same, their circumferences the smallest, and the circumference of the middle section the biggest. Let t_1 denote the circumferences of the upper and the lower sections and t_2 refer to the circumference of the middle section.

The curve shape of the ideal symmetric curve surface in the height direction keeps consistent. The projection curve L formed by the projection of the curve surface on the XOY coordinates (See Figure 5) is first considered to derive an equation. The parameters of the projection curve L can be written as follows:

$$\begin{cases} x = \varphi(t) \\ y = \phi(t) \end{cases} \quad (5)$$

Figure 6 illustrates the micro schematic diagram of the SE vector corresponding to the i th micro plain S_i . Let the angle between the micro plain S_i and axis X be α_i , the SE vector be vertical to the micro plane, and the angle between the SE vector and the axis Y be α_i . The vector SE_i is decomposed into two vectors on the direction X and direction Y (See Figure 6) to derive the comprehensive action of the SE vectors of all micro plains on the curve surface. The two vectors are denoted as SE_{xi} and SE_{yi} , respectively.

According to Figure 6, the angle α_i can be calculated as follows:

$$\tan \alpha_i = \frac{Y'_i}{X'_i} = \frac{\phi'(t_i)}{\varphi'(t_i)} \quad (6)$$

$$\sin \alpha_i = \frac{\phi'(t_i)}{\sqrt{\phi'^2(t_i) + \varphi'^2(t_i)}} \quad (7)$$

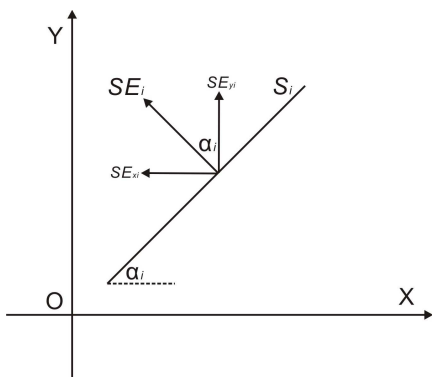


Figure 6. SE vector decomposition of the micro plain.

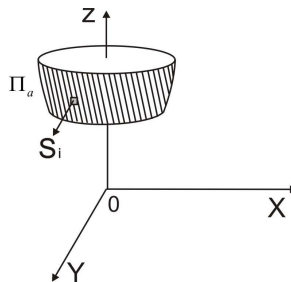


Figure 7. Idea curve model of the abdomen.

$$\cos \alpha_i = \frac{\phi'(t_i)}{\sqrt{\phi'^2(t_i) + \varphi'^2(t_i)}} \tag{8}$$

That is:

$$SE_{xi} = SE \frac{\phi'(t_i)}{\sqrt{\phi'^2(t_i) + \varphi'^2(t_i)}} \tag{9}$$

$$SE_{yi} = SE \frac{\varphi'(t_i)}{\sqrt{\phi'^2(t_i) + \varphi'^2(t_i)}} \tag{10}$$

Let SE_x and SE_y refer to the comprehensive SE of the section t on the directions of X and Y , respectively. λ is the reciprocal of the n , and the vectors SE_x and SE_y can be expressed as follows:

$$SE_x = \frac{\lim_{\lambda \rightarrow 0} SE \cdot \sum_{i=1}^n \sin \alpha_i \cdot \Delta S_i}{n} = \frac{SE[\phi(t_2) - \phi(t_1)]}{n} \tag{11}$$

$$SE_y = \frac{\lim_{\lambda \rightarrow 0} SE \cdot \sum_{i=1}^n \cos \alpha_i \cdot \Delta S_i}{n} = \frac{SE[\varphi(t_2) - \varphi(t_1)]}{n} \tag{12}$$

The whole curve surface Π is further considered. Let SE_x and SE_y be the SE vectors of the curve surface Π on the directions of X and Y , and the coordinates of upper and lower sections of the curve surface on the axis Z are t_1 and t_2 , respectively. The vectors of SE_x and SE_y can be calculated as follows:

$$SE_X = \int_{\omega(t_1)}^{\omega(t_2)} SE_x dz = \frac{SE[\phi(t_2) - \phi(t_1)]}{n} dz \tag{13}$$

$$SE_Y = \int_{\omega(t_1)}^{\omega(t_2)} SE_y dz = \frac{SE[\varphi(t_2) - \varphi(t_1)]}{n} dz \quad (14)$$

Let SE_T denote the comprehensive SE of the point O on the whole curve surface, which can be expressed as follows:

$$SE_T = \sqrt{SE_X^2 + SE_Y^2} \quad (15)$$

4. APPLICATION EXAMPLES OF COMPUTATION MODEL

According to the common model mentioned above, we take the waist and abdomen of the body for example to discuss the SE of the fabric under a symmetric curve condition. As shown in Figure 7, the local curve surface of the waist and the abdomen of the body is considered as an idea part of an elliptic surface, which is noted as Π_a . The local curve surface consists of enormous elliptic surfaces with different sizes on the direction of axis Z . The vertex of the elliptic surface is considered as the origin of the space coordinates. As for any section t , its circumference is L , the length of long axis is a , the length of the short axis is b , so the relation can be written as: $L = 2\pi b + 4(a - b)$.

Let the direction of the body width be the direction of the axis X , the direction of the body thickness be the direction of axis Y , and the direction of the incident wave be consistent with the direction of the body thickness. The curve surface is divided into n micro plains (ΔS_i). SE_i denotes the SE of the micro plain ΔS_i , its direction is vertical to the micro plain, $\cos \alpha_i$, $\cos \beta_i$ and $\cos \gamma_i$ are the cosine of the angles between the SE_i and the axis of X , Y and Z , respectively. According to the definition of the elliptic cone, the Π_a can be expressed as follows:

$$\frac{x^2}{a^2} + \frac{y^2}{b^2} = z^2 \quad (16)$$

If $z = t$, the Π_a can be rewritten as follows:

$$\frac{x^2}{(at)^2} + \frac{y^2}{(bt)^2} = 1 \quad (17)$$

Figure 8 shows the projection of the curve section on the coordination XOY when the z is equal to the t .

Where, the coordinates of four points P_1 , P_2 , P_3 and P_4 are $p_1(a_t, 0, t)$, $p_2(-a_t, 0, t)$, $p_3(0, b_t, t)$, $p_4(0, -b_t, t)$.

According to the principle mentioned above, for any section t , the SE_{xi} and SE_{yi} can be obtained as follows:

$$SE_{xi} = SE_i \frac{x_i}{\sqrt{a_t^4 z_i^2 + x_i^2 + \frac{a_t^4}{b_t^4} y_i^2}} \quad (18)$$

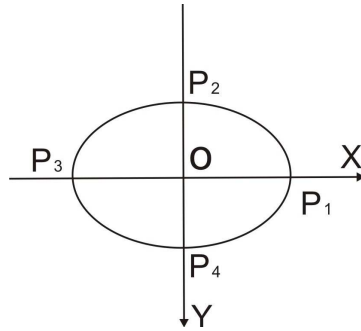


Figure 8. Curve projections on the coordination XOY .

$$SE_{yi} = SE_i \frac{y_i}{\sqrt{b_t^4 z_i^2 + y_i^2 + \frac{a_t^4}{b_t^4} x_i^2}} \tag{19}$$

A value range of a , b and z of all sections in the whole model can be obtained according to the Equations (18) and (19) and the actual size of the body’s abdomen. The final values of SE_x and SE_y can be calculated using the Equations (11)–(14). Considering the speed of the calculation, we write the program with MATLAB7.0. Figure 9 lists the detail steps.

5. EXPERIMENTS FOR MODEL VERIFICATION

5.1. Experimental Methods and Materials

We make a simulation local model of the human body to verify the proposed model, as shown in Figure 10. The inner part of the model is hollow. The SE value of the center point on the section is tested. The center point is selected from a health view, which is the center point of the abdomen of the human body. There are many organs in the body abdomen. Protection of this part is more than that of the skin. The simulation local model consists of metal sheet, which can shield the electromagnetic wave and its structure is semi-enclosed and hollow. A miniature signal receiver probe is installed on the center position of the model enclosed surface. The testing surface (non-enclosed surface) can be covered by the EMS fabric. The fabric can be formed a symmetric curve surface shape through a plastic cloth supporting circle. Experiments are conducted in an EMS chamber, as shown in Figure 11. A transmitting antenna which can transmit signals with different frequencies is placed in front of the simulation partial

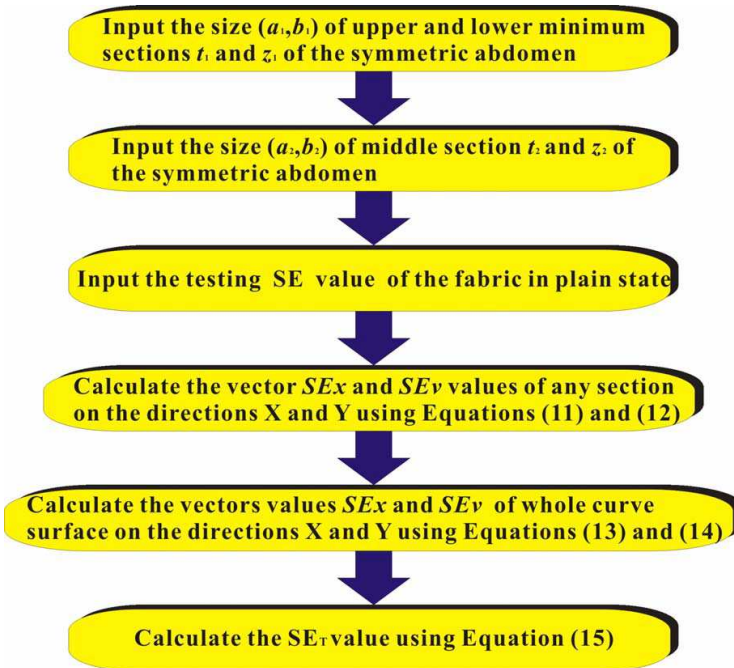


Figure 9. Computation flowchart.

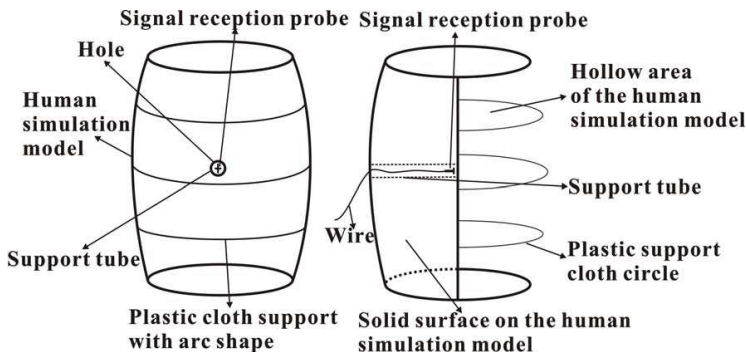


Figure 10. The face of simulation local model of human body.

model. A reception probe in the model is connected to a network analyzer to record data, which provide the basis for SE calculation. The SE of the model without covering the EMS fabric is tested, and the SE of the model with covering EMS fabric is then tested. The SE on the center position of the simulation model is calculated using Equation (1).

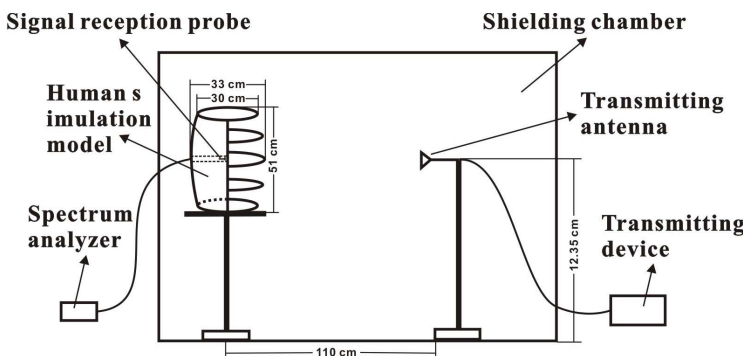


Figure 11. Testing schematic diagram.

Table 1. SE of fabric in a plain state under different frequencies.

Frequency (GHz)	0.6	0.8	1.0	1.2	1.4	1.6	1.8
SE (dB)	38.9	38.3	37.6	37	36.5	35.8	35.2

The testing fabric specifications are as follows: the material is stainless steel/cotton blended EMS fabric; Metal content is 15%; Fabric is provided by Shanghai Angel Textile Company.

The fabric SE in a plain state is tested every 0.2 GHz in the frequency range of 0.6 GHz–1.8 GHz using waveguide tube testing system, and the testing results are presented in Table 1.

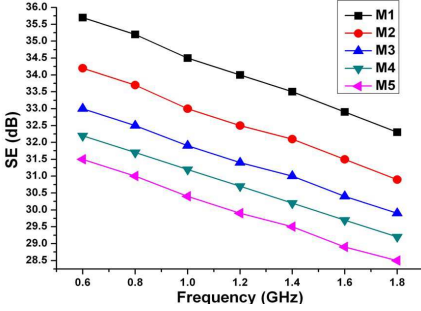
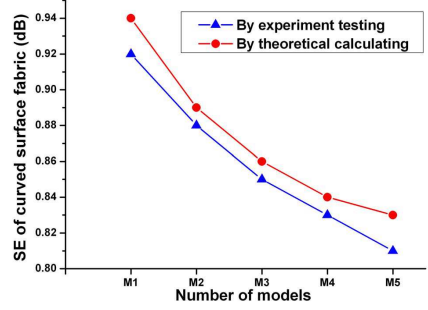
5.2. Testing Results

We make five simulation symmetric local models for experiments. The position of the model with the minimum circumference is the waist. The lengths of semi-long axis and semi-short axis of the section are $[a_1, b_1]$. The position of the model with the maximum circumference is the abdomen and the lengths of semi-long axis and semi-short axis of the section are $[a_2, b_2]$. The size difference between each two models is 10%, and models are numbered as M1, M2, M3, M4, M5. Table 2 presents the detailed sizes of the human models.

The human models are covered by the stainless steel/cotton blended EMS fabrics used in above experiments. The transmitting signals frequencies are selected from 0.6 GHz to 1.8 GHz. The fabric SE values of five different sizes human models are tested in every 0.2 GHz. Figure 12 illustrates the testing results.

Table 2. Sizes of different human models.

Human model number	Waist size (a_1, b_1) (cm)	Abdomen size (a_2, b_2) (cm)	Height of human model (cm)
M1	(24.3, 19.4)	(20.25, 14.6)	34.0
M2	(27.0, 21.6)	(22.5, 16.2)	34.0
M3	(30.0, 24.0)	(25.0, 18.0)	34.0
M4	(33.0, 26.4)	(27.5, 19.8)	34.0
M5	(36.3, 29.0)	(30.3, 21.8)	34.0

**Figure 12.** SE of five human models under different frequencies.**Figure 13.** SE comparisons of the symmetric curve surface between the testing value and the theoretical value.

As can be seen in Figure 12, for each human model, the SE decreases linearly with the increase of frequency. When the emission frequency is an arbitrary value, the ratio between the fabric SE (SE_T) of the five human models and the fabric SE (SE) in the plain state is always a constant. Let a refer to the constant and can be calculated by:

$$a = \frac{SE_T}{SE} \quad (20)$$

We also notice from Figure 12 that the SE difference between different sizes of human models is the same. Table 3 presents the ratio a between the value of SE_T and the value of SE according to the data from Figure 12.

Table 3. Ratio a value of different sizes human models.

Human model number	M1	M2	M3	M4	M5
a	0.92	0.88	0.85	0.83	0.81

Table 4. Theoretical SE value of different models using computation model.

Human model number	SE_X	SE_Y	SE_T
M1	0.75	0.57	0.94
M2	0.7	0.55	0.89
M3	0.67	0.54	0.86
M4	0.61	0.58	0.84
M5	0.56	0.61	0.83

Table 5. Deviation rate between the testing value and the theoretical value.

Deviation rate	M1	M2	M3	M4	M5
δ	2.17%	1.14%	1.18%	1.20%	2.47%

6. ANALYSES

6.1. Theoretical Computation Results

The SE values of the centre point of the five models covered the EMS fabric are calculated using Equations (16)–(19) and the computation program in Figure 9. Table 4 lists the computation results.

6.2. Deviation Rate between Testing Value and Theoretical Value

A deviation rate is introduced to analyze the comparison between the testing data and the theoretical data. Let $SE_{T,T}$ denote the testing data and $SE_{T,C}$ represent the theoretical data, and the deviation rate δ can be expressed as follows:

$$\delta = \frac{SE_{T,C} - SE_{T,T}}{SE_{T,T}} \times 100\% \tag{21}$$

Table 5 presents the deviation rate between the testing data and the theoretical data according to Tables 3 and 4.

6.3. Variations between the Testing Value and the Theoretical Value

A SE comparison between the testing value and the theoretical value is conducted according to Tables 3 and 4 to discuss the SE variations of the symmetric curve surface, as shown in Figure 13.

As can be seen from Figure 13, it can be concluded as follows:

(1) There is a certain SE deviation between the testing value and the theoretical value. The theoretical value is more than the testing value. The deviation rate is less than 3% according to the computations in Table 5.

(2) There is a close area between the theoretical value curve and the testing value curve. The phenomenon indicates the deviation rate is little. For example, for model M2 and model M3, the left and right curves are far, the deviation rate is big. It indicates that there is a best region which the deviation rate is least among the theoretical values.

(3) The theoretical values or the testing values of the SE are inversely proportional to the curvature of curve fabric. The curvature value is bigger, and the SE value is lower.

6.4. Deviation Reasons Analyses

The main reasons result in the results in Table 5 and Figure 13 as follows:

(1) When the theoretical SE value is calculated, we suppose that the electromagnetic wave incidents into the curve fabric with one direction, no considering other directions. In actual testing, the SE value is obtained from the stimulated human model which has many surfaces. Other more tiny electromagnetic waves may be leaked because of the EMS chamber or the fabric. The SE value from actual testing is lower than that from theoretical calculation.

(2) When the curvature of the curve fabric is larger or less than a certain value, the difference between the theoretical value and the testing value is bigger and bigger. Therefore, the application of the theoretical model possesses a certain range. The reason is the arrangement of the stain steel fiber. When the curvature of the curve fabric is larger than a value, the arrangement of the stainless steel fiber will produce uneven phenomenon, and the interstices among fibers increase. However, the theoretical values are obtained on the premise of even fabric. Thus, the deviation is large. When the curvature of the curve fabric is less than a value, the fabric is near to a plain state. The SE value is calculated by curve equations results in inaccurate results.

(3) When the curve fabric is blended, the fabric produces tiny change, mainly is the interstices increase among metal fibers, making

the transmission probabilities of the electromagnetic wave are added. The curve surface is obvious, the number of interstices is added result in the SE values decline. The SE variations of the stimulation model show that $M1 > M2 > M3 > M4 > M5$.

7. CONCLUSIONS

(1) Theoretical analyses and experiments proved that the comprehensive SE computation base on the SE vector is correct and feasible. The comprehensive SE can be calculated by the characteristics of the curve surface fabric.

(2) The proposed computation model can calculate the SE of the clothing partial, and the deviation between the computation value and the testing value is less than 3%. The symmetric local possesses a size range. In this range, the deviation between the computation value and the testing value is the least.

(3) The deviation between the computation value and the testing value is related to the tightness degree of the fabric covering and the curvature of the curve surface. The SE value is inversely proportional to the size of the shielding fabric.

REFERENCES

1. Wang, J. and Z. Xi, "Research progress of electromagnetic shielding material of metal fiber," *Rare Metal Materials and Engineering*, Vol. 40, 1688–1692, 2011.
2. Sun, R. J., K. Lai, and J. C. Zhang, "Suggestion on the test for electromagnetic shielding in the fabric for costume," *Journal of Xian University of Engineering Science and Technology*, Vol. 17, No. 2, 100–103, 2003.
3. Schmid, E., W. Panzer, H. Schlattl, and H. Eder, "Emission of fluorescent x-radiation from non-lead based shielding materials of protective clothing: A radiobiological problem?," *Journal of Radiological Protection*, Vol. 32, No. 3, 29–39, 2012.
4. Zhu, X. Y., X. J. Li, and B. K. Sun, "Study on electromagnetic shielding efficacy of knitting clothing," *Przegląd Elektrotechniczny*, Vol. 88, No. 3B, 42–43, 2012.
5. Kurokawa, S. and T. Sato, "A design scheme for electromagnetic shielding clothes via numerical computation and time domain measurements," *IEICE Transactions on Electronics*, Vol. E86C, No. 11, 2216–2223, 2003.

6. Yoshimura, Y., I. Nagano, S. Yagitani, T. Ueno, and T. Nakayabu, "FDTD analysis of effectiveness of shielding clothes in suppressing electromagnetic field in phantom model," *Transactions of the Institute of Electrical Engineers of Japan*, Vol. 123, No. 7, 623–629, 2003.
7. Wang, X. C. and Z. Liu, "Shielding efficiency mathematics model on the electromagnetic shielding clothing," *Journal of Textile Research*, Vol. 29, 73–75, 2008.
8. Li, R., L. Zhang, and L. Jia, "Influence of fabric structural model on shielding effectiveness of electromagnetic radiation shielding fabric," *Int. J. Modeling, Identification and Control*, Vol. 11, Nos. 3–4, 211–217, 2010.
9. Jayasree, P. V. Y., V. S. S. N. S. Baba, B. Prabhakar Rao, and P. Lakshman, "Analysis of shielding effectiveness of single, double and laminated shields for oblique incidence of em waves," *Progress In Electromagnetics Research B*, Vol. 22, 187–202, 2010.
10. Hakansson, E., A. Amie, and A. Kaynak, "Dielectric characterization of conducting textiles using free space transmission measurements: Accuracy and methods for improvement," *Synthetic Metals*, Vol. 157, 1054–1063, 2007.
11. Ortlek, H. G., O. G. Saracoglu, O. Saritas, and S. Bilgin, "Electromagnetic shielding characteristics of woven fabrics made of hybrid yarns containing metal wire," *Fibers and Polymers*, Vol. 13, No. 1, 63–67, 2012.
12. Wang, X. C. and Z. Liu, "A new computation of shielding effectiveness of electromagnetic radiation shielding fabric," *Progress In Electromagnetics Research Letters*, Vol. 33, 177–186, 2012.
13. Osman, M. A. R., M. K. A. Rahim, N. A. Samsuri, H. A. M. Salim, and M. F. Ali, "Embroidered fully textile wearable antenna for medical monitoring applications," *Progress In Electromagnetics Research*, Vol. 117, 321–337, 2011.
14. Ching, I. S. and T. C. Jin, "Effect of stainless steel-containing fabrics on electromagnetic shielding effectiveness," *Textile Res. J.*, Vol. 74, No. 1, 51–54, 2004.
15. Liu, Z. and X. C. Wang, "Influence of fabric weave type on the effectiveness of electromagnetic shielding woven fabric," *Journal of Electromagnetic Waves and Applications*, Vol. 26, Nos. 14–15, 1848–1856, 2012.
16. Raj, C. D., G. S. Rao, P. V. Y. Jayasree, B. Srinu, and P. Lakshman, "Estimation of reflectivity and shielding effectiveness of three layered laminate electromagnetic shield at

- X-band,” *Progress In Electromagnetics Research B*, Vol. 20, 205–223, 2010.
17. Mao, Y., B. Chen, H. Q. Liu, J. L. Xia, and J.-Z. Tang, “A hybrid implicit-explicit spectral FDTD scheme for oblique incidence problems on periodic structures,” *Progress In Electromagnetics Research*, Vol. 128, 153–170, 2012.
 18. Wu, G., X. Zhang, Z. Q. Song, and B. Liu, “Analysis on shielding performance of metallic rectangular cascaded enclosure with apertures,” *Progress In Electromagnetics Research Letters*, Vol. 20, 185–195, 2011.
 19. Zhao, Y., F. Chen, H. Chen, N. Li, Q. Shen, and L. Zhang, “The microstructure design optimization of negative index metamaterials using genetic algorithm,” *Progress In Electromagnetics Research Letters*, Vol. 22, 95–108, 2011.
 20. Qian, Z. and Z. J. Chen, *Electromagnetic Compatibility Design and Interference Suppression Technology*, Zhejiang University Press, Hangzhou, 2000.